Available online at www.sciencedirect.com

ScienceDirect

Energy Procedia 158 (2019) 1666–1671

Energy Procedia

www.elsevier.com/locate/procedia

10th International Conference on Applied Energy (ICAE2018), 22-25 August 2018, Hong Kong, China

Modeling of a combined CH_4-assisted solid oxide co-electrolysis and Fischer-Tropsch synthesis system for low-carbon fuel production

Haoran Xu[a], M. Mercedes Maroto-Valer[a,*], Meng Ni[b], Jun Cao[c], Jin Xuan[d,*]

[a]*Research Centre for Carbon Solutions (RCCS), School of Engineering & Physical Sciences, Heriot-Watt University, Edinburgh, EH14 4AS, United Kingdom*

[b]*Building Energy Research Group, Department of Building and Real Estate, The Hong Kong Polytechnic University, Hung Hom, Kowloon, Hong Kong, China*

[c]*State Key Laboratory of Chemical Engineering, School of Mechanical and Power Engineering, East China University of Science and Technology, Shanghai, China*

[d]*Department of Chemical Engineering, Loughborough University, Loughborough, United Kingdom*

Abstract

CH_4-assisted solid oxide electrolyzer cells (SOECs) can co-electrolyze H_2O and CO_2 effectively for simultaneous energy storage and CO_2 utilization. Compared with conventional SOECs, CH_4-assisted SOECs consume less electricity because CH_4 in the anode provides part of the energy for electrolysis. As syngas (CO and H_2 mixture) is generated from the co-electrolysis process, it is necessary to study its utilization through the subsequent processes, such as Fischer-Tropsch (F-T) synthesis. An F-T reactor can convert syngas into hydrocarbons, and thus it is very suitable for the utilization of syngas. In this paper, the combined CH_4-assisted SOEC and F-T synthesis system is numerically studied. Validated 2D models for CH_4-assisted SOEC and F-T processes are adopted for parametric studies. It is found that the cathode inlet H_2O/ CO_2 ratio in the SOEC significantly affects the production components through the F-T process. Other operating parameters such as the operating temperature and applied voltage of the SOEC are found to greatly affect the productions of the system. This model can be used for understanding and design optimization of the combined fuel-assisted SOEC and F-T synthesis system to achieve economical hydrocarbon generation.

Keywords: Solid oxide electrolyzer cell; Fischer-Tropsch synthesis; Mathematical modeling; Hydrocarbon generation

* Corresponding authors. Tel.: +44 (0)131 451 3293; fax: +44 (0)131 451 3293.
E-mail address: m.maroto-valer@hw.ac.uk (MMV); j.xuan@lboro.ac.uk (JX)

1876-6102 © 2019 The Authors. Published by Elsevier Ltd.
This is an open access article under the CC BY-NC-ND license (http://creativecommons.org/licenses/by-nc-nd/4.0/)
Peer-review under responsibility of the scientific committee of ICAE2018 – The 10th International Conference on Applied Energy.
10.1016/j.egypro.2019.01.388

1. Introduction

With the growing attention on global warming, effective CO_2 utilization methods are urgently needed. Solid oxide electrolyzer cells (SOECs) are promising technologies to convert CO_2 into chemical fuels such as CO. Compared with low-temperature electrolyzers, SOECs consume less electrical energy as part of the input energy comes from heat. The high operating temperature also allows the use of non-noble catalysts in the SOEC, leading to a lower overall cost. Recently, the concept of fuel-assisted SOECs has been demonstrated, where low-cost fuels (e.g. methane) are supplied to the anode to reduce the operating potentials of the SOEC [1]. The fuel-assisted SOECs can even electrolyze oxidants without consuming electricity, which means it is possible to convert CO_2 to fuels by only consuming low-cost fuels in the SOEC [2].

SOECs can co-electrolyze H_2O and CO_2 and generate syngas (H_2 and CO mixture), which can be further utilized in the Fischer-Tropsch (F-T) reactor for low carbon fuel production [3, 4]. As methane is usually less wanted from the F-T synthesis process, it is therefore suitable to use methane as the assistant fuel in the SOEC for CO_2 and H_2O co-electrolysis. A system consisting of a CH_4-assisted SOEC and a F-T reactor is very promising for CO_2 utilization and hydrocarbon fuel generation. However, despite some preliminary studies on the combined SOEC and F-T systems [5, 6], no study on a combined fuel-assisted SOEC and F-T reactor system has been conducted thus far. To fill this research gap, in this work 2D mathematical models are developed for a combined CH_4-assisted SOEC and F-T reactor system for H_2O/CO_2 co-electrolysis and hydrocarbon fuel generation. The sub-models for the CH_4-assisted SOEC and the F-T reactor are validated in the previous studies [7, 8]. Parametric simulations are conducted to understand the characteristics of such a system and the interplay of different physical/chemical processes.

2. Model description

The proposed hybrid system consists of a CH_4-assisted SOEC and a F-T reactor, as shown in Fig. 1. In the SOEC anode, CH_4 and H_2O are supplied to anode with a ratio of 1:1.5 to avoid methane coking. CO_2 and H_2O are supplied to the cathode, where they are electrolyzed to generate syngas. Syngas generated from the SOEC section is collected for F-T reactor, where hydrocarbons are generated through the synthesis process.

2D numerical models are developed to simulate the characteristics of the system, the model kinetics for both the CH_4-assisted SOEC and the F-T reactor are validated by using prior published work [7, 8]. The tubular SOEC has a length of 7 cm, an inner diameter of 0.3 cm and an outer diameter of 0.5 cm. It uses Ni-YSZ as anode support layer, Ni-ScSZ as anode active layer, ScSZ as electrolyte and Ni-ScSZ as cathode. The tubular F-T reactor has a length of 30 cm and an outer diameter of 1cm. It uses Fe based catalyst for the improvement of synthesis reaction rates. The material properties for the SOEC can be found in Table 1.

For model simplification, the following assumptions are adopted:

1. The electrochemical reaction active sites are assumed to be uniformly distributed in the porous electrodes.
2. The electronic and ionic conducting phases are continuous and homogeneous in the porous electrodes.
3. All the gases are considered as ideal gases.
4. Temperature distribution is uniform in the reactors due to the small size.

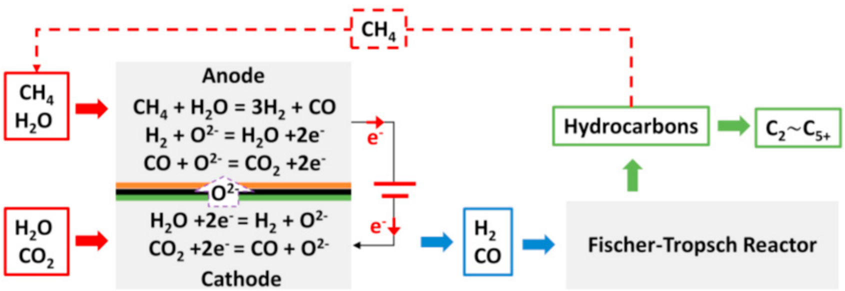

Fig. 1. Schematic of combined CH_4-assisted SOEC and F-T reactor system

Table 1. Material properties.

Parameters	Value or expression	Unit
σ_{ScSZ}	$69200 \times e^{\frac{-9681}{T}}$	S m^{-1}
σ_{YSZ}	$33400 \times e^{\frac{-10300}{T}}$	S m^{-1}
σ_{Ni}	$4.2 \times 10^6 - 1065.3T$	S m^{-1}
ε	0.36	
τ	3	
S_{TPB}	2.14×10^5	m^{-1}

2.1. Sub-model of CH_4-assisted SOEC for CO_2 and H_2O co-electrolysis

As shown in Fig. 1, the gas mixture of H_2O and CO_2 flows into the cathode channel, while the gas mixture of CH_4, and H_2O flows into the anode channel. In the cathode, both H_2O and CO_2 are reduced to generate H_2 and CO as shown in Eq. (1) and Eq. (2), respectively.

$$H_2O + 2e^- = H_2 + O^{2-} \tag{1}$$

$$CO_2 + 2e^- = CO + O^{2-} \tag{2}$$

In the anode, the methane steam reforming (MSR) reaction happens to generate H_2 and CO, which are then electrochemically oxidized by the O^{2-} transported from the cathode. The MSR reaction and electrochemical oxidizations of H_2 and CO are listed as shown in Eq. (3) to Eq. (5).

$$CH_4 + H_2O = CO + 3H_2 \tag{3}$$

$$H_2 + O^{2-} = H_2O + 2e^- \tag{4}$$

$$CO + O^{2-} = CO_2 + 2e^- \tag{5}$$

Due to the existence of H_2O and CO, water gas shift reaction (WGSR) occurs in both anode and cathode as

$$CO + H_2O = CO_2 + H_2 \; . \tag{6}$$

In operation, the required voltage applied to SOEC can be calculated by Eq. (7):

$$V = E + \eta_{act} + \eta_{ohmic} \; , \tag{7}$$

where E is the equilibrium potential related with thermodynamics; η_{act} is the activation overpotentials reflecting the electrochemical activities and η_{ohmic} is the ohmic overpotential calculated by the Ohmic law.

The calculation of equilibrium potential is based on oxygen partial pressure [9] and calculated as:

$$E = \frac{RT}{nF} \ln\left(\frac{\sum P^L_{O_2,ca}}{\sum P^L_{O_2,an}}\right), \tag{8}$$

where R is the universal gas constant (8.3145 J mol^{-1} K^{-1}), T is temperature (K), F is the Faraday constant (96485 C mol^{-1}), n is the number of electrodes transferred per electrochemical reaction, $P^L_{O_2,ca}$ and $P^L_{O_2,an}$ are oxygen partial pressures in the cathode and anode, respectively.

For the pairs of H_2O/H_2 and CO_2/CO, their oxygen partial pressures can be expressed by:

$$P^L_{O_2,(H_2O/H_2)} = \left(\frac{P^L_{H_2O}}{P^L_{H_2}} \cdot e^{\frac{\Delta G_{H_2O/H_2}}{RT}}\right)^2, \text{ and} \tag{9}$$

$$P^L_{O_2,(CO_2/CO)} = \left(\frac{P^L_{CO_2}}{P^L_{CO}} \cdot e^{\frac{\Delta G_{CO_2/CO}}{RT}}\right)^2 , \tag{10}$$

where $P^L_{H_2O}$, $P^L_{H_2}$, $P^L_{CO_2}$ and P^L_{CO} are local partial pressures of H_2O, H_2, CO_2 and CO, respectively. $\Delta G_{H_2O/H_2}$ and $\Delta G_{CO_2/CO}$ are the Gibbs free energy change in the H_2 and CO oxidation reactions, respectively.

The activation overpotential is calculated by the Butler-Volmer eqution

$$i = i_0 \left\{\exp\left(\frac{\alpha nF\eta_{act}}{RT}\right) - \exp\left(\frac{-(1-\alpha)nF\eta_{act}}{RT}\right)\right\}, \tag{11}$$

where i_0 is the exchange current density and α is the electronic transfer coefficient. For H_2O electrolysis, the exchange current density can be further expressed as

$$i_0 = \beta \frac{P_{H_2O}}{P_{ref}} \frac{P_{H_2}}{P_{ref}} \exp\left(-\frac{E_a}{RT}\right), \tag{12}$$

where β is the activity factor and E_a is the activation energy. For CO_2 electrolysis, its exchange current density is 0.45 times of H_2O electrolysis [10]. All the kinetics for above reactions can be found in Table 2.

Table 2. Reaction kinetic parameters

Parameters	Value or expression	Unit
β	3.3×10^{8}	Am^{-2}
E_a	1.2×10^{5}	$J\ mol^{-1}$
α_{H_2O}	0.65	
α_{CO_2}	0.65	
R_{MSR} [11]	$k_{rf}(p_{CH_4}p_{H_2O}-\frac{p_{H_2}^3 p_{CO}}{K_{pr}})$	$mol\ m^{-3}\ s^{-1}$
k_{rf}	$2395\exp(\frac{-231266}{RT})$	$mol\ m^{-3}\ Pa^{-2}\ s^{-1}$
K_{pr}	$1.0267\times 10^{10}\exp(-0.2513Z^4+0.3665Z^3+0.5810Z^2-27.134Z+3.277)$	
R_{WGSR} [12]	$k_{sf}(p_{H_2O}p_{CO}-\frac{p_{H_2}p_{CO_2}}{K_{ps}})$	$mol\ m^{-3}\ s^{-1}$
k_{sf}	$0.0171\exp(\frac{-103191}{RT})$	$mol\ m^{-3}\ Pa^{-2}\ s^{-1}$
K_{ps}	$\exp(-0.2935Z^3+0.6351Z^2+4.1788Z+0.3169)$	
Z	$\frac{1000}{T}-1$	

2.2. Sub-model of F-T reactor

The F-T reactor uses Fe-HZSM5 as catalyst and works at 573 K and 2 MPa for syngas synthesis. The reactions in the F-T process are shown in Eq. (13) to Eq. (20).

$$CO+3H_2=CH_4+H_2O \tag{13}$$
$$2CO+4H_2=C_2H_4+2H_2O \tag{14}$$
$$2CO+5H_2=C_2H_6+2H_2O \tag{15}$$
$$3CO+7H_2=C_3H_8+3H_2O \tag{16}$$
$$4CO+9H_2=n-C_4H_{10}+4H_2O \tag{17}$$
$$4CO+9H_2=i-C_4H_{10}+4H_2O \tag{18}$$
$$6.05CO+12.23H_2=C_{6.05}H_{12.36}(C_5+)+6.05H_2O \tag{19}$$
$$CO+H_2O=CO_2+H_2 \tag{20}$$

The reaction kinetics for above reactions can be expressed as [8]

$$R_i=0.278k_i\exp(-\frac{E_i}{RT})P_{CO}^{m}\cdot P_{H_2}^{n}, \tag{21}$$

2.3. CFD Sub-model

For both the SOEC and the F-T reactor, the mass transport of gas species is calculated by extended Fick's law

$$N_i=-\frac{1}{RT}\left(\frac{B_0 y_i P}{\mu}\nabla P-D_i^{eff}\nabla(y_i P)\right)\ (i=1,\dots,n), \tag{22}$$

where B_0 is the material permeability, μ is the gas viscosity, y_i and D_i^{eff} are the mole fraction and effective diffusion coefficient of component i, respectively. D_i^{eff} can be further determined by

$$D_i^{eff}=\frac{\varepsilon}{\tau}\left(\frac{1}{D_{im}^{eff}}+\frac{1}{D_{ik}^{eff}}\right)^{-1}, \tag{23}$$

where ε is the porosity, τ is the tortuosity factor, D_{im}^{eff} is the molecular diffusion coefficient and D_{ik}^{eff} is the Knudsen diffusion coefficient [13].

The mass conservation can be described by

$$\nabla\left(-D_i^{eff}\nabla c_i\right)=r_i, \tag{24}$$

where c_i is the gas molar concentration and r_i is the mass source term of the gaseous species.

Navier-Stokes equation with Darcy's term is adopted to calculate the momentum transport in both the SOEC and F-T reactor as shown in Eq. (25).

$$\rho \frac{\partial u}{\partial t} + \rho u \nabla u = -\nabla p + \nabla\left[\mu\left(\nabla u + (\nabla u)^T\right) - \frac{2}{3}\mu \nabla u\right] - \frac{\varepsilon \mu u}{k} \tag{25}$$

Here ρ is the gas density and u is the velocity vector.

2.4. Boundary conditions and model solution

Electric potentials are specified at the outer surface of two electrodes with the cell ends electrical insulated. Inlet gas flow rate and mole fraction of the species are given at inlets of the SOEC. The ratio of H_2 to CO for F-T reactor inlet is consistent with the ratio of H_2 to CO of SOEC cathode outlet. The numerical models are solved at given parameters using commercial software COMSOL MULTIPHYSICS®.

3. Results and discussions

As shown in Fig. 2(a), with the increase of SOEC operating temperature, the mole fractions of H_2 and CO in the outlets significantly increase due to the improved electrochemical activity. With the more complete conversion of CO_2 at higher temperatures, the ratio of outlet H_2/CO continuously decreases from ~8 to ~1, indicating the much-increased CO fraction in the generated syngas.

Besides, the applied voltage largely affects the performance of the SOEC, as shown in Fig. 2(b). Compared with traditional SOECs working at 1V ~3 V applied voltage, the CH_4-assisted SOEC performs well at a low applied voltage. The mole fraction of syngas in the outlet is closed to 1 at 0.7 V and the cell can even work at 0 V applied voltage with the driven force provided by CH_4 in the anode, which means no input electrical power is needed. Therefore, the SOEC offers a high conversion rate while only consume very limited electricity benefited from methane assistance.

The characteristic of C_nH_m production with the change of inlet H_2/CO ratio from the F-T reactor is shown in Fig. 2(c), where the mole fraction of both total hydrocarbons and CH_4 are found to be improved with the increase of inlet H_2 mole fraction. For comparison, the outlet mole fractions of C_2H_6, C_3H_8 and C_{5+} show slightly increase at higher inlet H_2 mole fraction, while nearly no changed is found on the outlet mole fractions of C_2H_4 and C_4H_{10}.

Finally, the mole fractions of low-carbon fuels production from the F-T reactor with the change of inlet H_2O/CO_2 ratio of the CH_4-assisted SOEC is shown in Fig. 2(d). At small H_2O/CO_2 ratio (0.3: 0.7) for SOEC inlet, the F-T reactor generates 4 times $C_2 \sim C_{5+}$ as much as CH_4. When the H_2O/CO_2 ratio increases 0.5: 0.5, the outlet $C_2 \sim C_{5+}$ and CH_4 also comes to a similar level. At the 0.6: 0.4 H_2O/CO_2 ratio, CH_4 generated by the F-T reactor becomes much larger than $C_2 \sim C_{5+}$ with a ratio close to 2: 1.

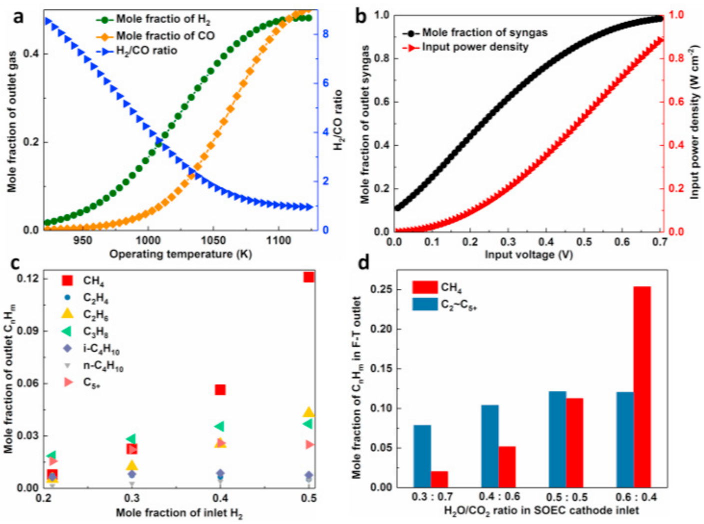

Fig. 2. (a, b) The effects of SOEC operating parameters on its performance; (c) the effects of F-T reactor inlet H_2/CO ratio on its outlet hydrocarbon components; (d) the effect of SOEC inlet H_2O/CO_2 ratio on the outlet hydrocarbon components of the F-T reactor.

4. Conclusions

The first 2D model combining a CH_4-assisted solid oxide co-electrolysis and Fischer-Tropsch synthesis system for low-carbon fuel production is developed in this paper. The kinetics of the model are validated by using previous studies. CO_2 and H_2O are used as the raw materials in the SOEC section for the generation of low-carbon fuel through the F-T reactor. By conducting parametric studies, it is found that the operating temperature, the applied voltage and the inlet H_2O/CO_2 ratio significantly affect the outlet syngas components of SOEC, thus greatly affect the characteristics of the hydrocarbons synthesized by the F-T reactor. As a result, the mole fractions of CH4 and $C_2 \sim C_{5+}$ generated by the F-T reactor can be controlled by adjusting the inlet H_2O/CO_2 ratio in the electrolysis process. This study builds a solid foundation for the understanding and optimization of a combined fuel-assisted SOEC and F-T reactor system.

Acknowledgements

The research is supported by the UK Engineering and Physical Science Research Council (EPSRC) through grants EP/K021796/1 and EP/N009924/1.

References

[1] Luo Y, Shi Y, Li W, Ni M, Cai N. Elementary reaction modeling and experimental characterization of solid oxide fuel-assisted steam electrolysis cells. International Journal of Hydrogen Energy. 2014;39:10359-73.
[2] Xu H, Chen B, Ni M. Modeling of Direct Carbon-Assisted Solid Oxide Electrolysis Cell (SOEC) for Syngas Production at Two Different Electrodes. J Electrochem Soc. 2016;163:F3029-F35.
[3] Chen L, Chen F, Xia C. Direct synthesis of methane from CO2-H2O co-electrolysis in tubular solid oxide electrolysis cells. Energy & Environmental Science. 2014;7:4018-22.
[4] Chen B, Xu H, Chen L, Li Y, Xia C, Ni M. Modelling of One-Step Methanation Process Combining SOECs and Fischer-Tropsch-like Reactor. J Electrochem Soc. 2016;163:F3001-F8.
[5] Becker WL, Braun RJ, Penev M, Melaina M. Production of Fischer–Tropsch liquid fuels from high temperature solid oxide co-electrolysis units. Energy. 2012;47:99-115.
[6] Stempien JP, Ni M, Sun Q, Chan SH. Thermodynamic analysis of combined Solid Oxide Electrolyzer and Fischer–Tropsch processes. Energy. 2015;81:682-90.
[7] Xu H, Chen B, Irvine J, Ni M. Modeling of CH4-assisted SOEC for H2O/CO2 co-electrolysis. International Journal of Hydrogen Energy. 2016;41:21839-49.
[8] Rahimpour MR, Elekaei H. A comparative study of combination of Fischer–Tropsch synthesis reactors with hydrogen-permselective membrane in GTL technology. Fuel Processing Technology. 2009;90:747-61.
[9] Stempien JP, Liu Q, Ni M, Sun Q, Chan SH. Physical principles for the calculation of equilibrium potential for co-electrolysis of steam and carbon dioxide in a Solid Oxide Electrolyzer Cell (SOEC). Electrochimica Acta. 2014;147:490-7.
[10] Luo Y, Shi Y, Li W, Cai N. Comprehensive modeling of tubular solid oxide electrolysis cell for co-electrolysis of steam and carbon dioxide. Energy. 2014;70:420-34.
[11] Ni M. 2D heat and mass transfer modeling of methane steam reforming for hydrogen production in a compact reformer. Energy Conversion and Management. 2013;65:155-63.
[12] Ni M. An electrochemical model for syngas production by co-electrolysis of H2O and CO2. Journal of Power Sources. 2012;202:209-16.
[13] Suwanwarangkul R, Croiset E, Fowler MW, Douglas PL, Entchev E, Douglas MA. Performance comparison of Fick's, dusty-gas and Stefan–Maxwell models to predict the concentration overpotential of a SOFC anode. Journal of Power Sources. 2003;122:9-18.